Determination of Cs-Cs Interaction Parameters Using Feshbach Spectroscopy

Andrew J. Kerman, Cheng Chin, Vladan Vuletić, and Steven Chu

Department of Physics, Stanford University, Stanford, CA 94306-4060, USA
E-mail: jkerman@leland.stanford.edu

Paul. J. Leo, Carl J. Williams, and Paul S. Julienne

Atomic Physics Division, National Institute of Standards and Technology, Gaithersburg, MD 20899, USA

Abstract. We measure high-resolution Feshbach resonance spectra for ultracold cesium atoms colliding in different hyperfine and magnetic sublevels. More than 25 Feshbach resonances are observed for magnetic fields below 230 G in the elastic and inelastic ground state collision cross sections, as well as in the cross-section for light-assisted collisions. From these spectra a consistent set of ground state molecular interaction parameters for cesium is extracted, including singlet and triplet scattering lengths of $A_s = (280\pm10)a_0$ and $A_t = (2400\pm100)a_0$, a van der Waals coefficient $C_6 = (6890\pm35)$a.u., as well as the strength of the indirect spin-spin coupling. This set of parameters allows for the first time a complete characterization of cesium's ultracold collision properties.

Ultracold cesium collisions have been the subject of a large number of experimental [1–8] and theoretical [9–12] studies in recent years. Aside from its obvious importance as the source of our primary time and frequency standard, recent experiments have shown that ground state cesium exhibits anomalous collision properties, such as a zero-energy resonance [2] and extremely large dipolar relaxation rates [3,4]. These effects have important implications for the stability of laser-cooled cesium atomic clocks [5], precision measurements such as searches for T-violating effects beyond the standard model in atoms [13], as well as attempts to produce a cesium Bose-Einstein condensate [4].

In this paper we present high-resolution studies of these cold collision interactions using a technique we label Feshbach spectroscopy. This method exploits the fact that the threshold collision properties of a binary system are almost completely determined by the presence of molecular bound or virtual states near the threshold for dissociation. We probe these very weakly bound levels by tuning them into de-

generacy with the scattering continuum of a lower lying internal state of the atom pair using the relative Zeeman shift induced by an external magnetic field. When a bound level is resonant with colliding atom pairs, the elastic and inelastic collision cross-sections exhibit a resonance behavior first predicted by H. Feshbach in the context of nuclear scattering [14], and more recently by Verhaar and co-workers for cold atomic collisions [10]. These so-called Feshbach resonances are ubiquitous, and have been either predicted [10,11,15] or observed [6–8,16,17] to occur in virtually all of the alkali atomic species. Since Feshbach resonance spectroscopy involves only atoms in stable ground states, it has inherently high resolution, allowing us to precisely chart the positions of weakly bound molecular states, and from these measurements extract for the first time a self-consistent set of ground state molecular interaction parameters for cesium [8,12]. Possible implications for future atomic clocks and cesium Bose-Einstein condensation are discussed.

The apparatus used for these measurements has been described previously [6–8]. Samples of up to 2×10^8 cesium atoms are loaded into a far-detuned dipole trap from a vapor-cell MOT using 3D degenerate Raman sideband cooling in a 3D optical lattice [18] which is superimposed on the overlapping MOT and dipole trapping volume. Temperatures in the range of a few μK and densities above $10^{13}\mathrm{cm}^{-3}$ are produced in the dipole trap which is formed by a 20W single frequency Nd:YAG laser retroreflected upon itself to form a 1D optical lattice, which is sufficiently far detuned from resonance to make the spontaneous scattering rate of trap photons negligible. The lifetime of the atoms in this trap is background-gas pressure limited to about 2 seconds, providing ample time for sensitive collisional measurements. The number of atoms in the trap is measured by collecting resonance fluorescence onto a calibrated photodiode, the temperature of the sample is measured using a time-of-flight technique, and the trap vibration frequencies using parametric excitation [6–8].

We observe collisional processes in atomic samples polarized into several different magnetic sublevels of the cesium ground state. In all cases the atomic polarization is optimized with care, and polarization purities as high as 97% are achieved. First, we consider $|\mathrm{F}{=}3,\mathrm{m}{=}3\rangle$, into which the atoms are already polarized after Raman-sideband cooling. This is the lowest energy state in a magnetic field, and therefore it is stable against binary inelastic processes. We observe Feshbach resonances in the elastic collisions between these atoms by loading them into a shallow trap whose depth is comparable to their temperature, and monitoring the subsequent evaporative loss from the trap as a function of magnetic field. A large elastic cross-section results in a fast loss of atoms from the trap, while a small elastic cross-section produces a slow loss. Fig. 1(a) shows this evaporative loss over a fixed time interval as a function of magnetic field. Although this quantity is not a linear function of the elastic cross-section, it is still a monotonic function and provides higher signal-to-noise for the location of resonance features in the cross-section than previous methods using temperature measurements [6].

To prepare atoms in the $|3,{-}3\rangle$ state, which is of most interest for magnetic trapping and evaporative cooling [3,4], we quickly reverse the magnetic bias field

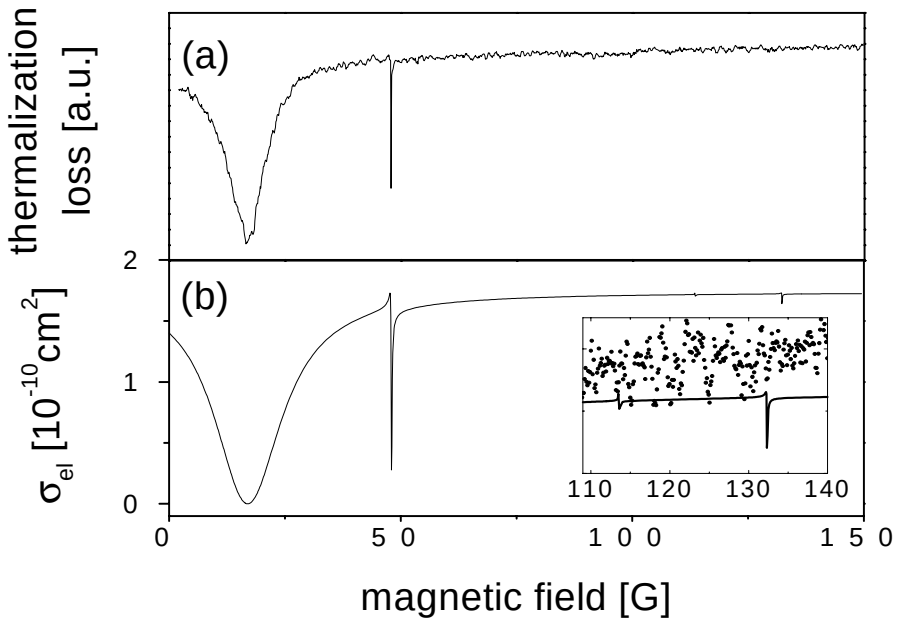

FIGURE 1. T(a) Elastic collision-induced loss rate from a shallow trap vs. magnetic field for the $|3,3\rangle$ state, which is stable against inelastic binary collisions. (b) Theoretical curve obtained by fitting to the resonance positions shown in Figs. 1(a), 2, and 3. The positions of the minima exactly match those in Fig. 1(a).

along which the atoms are polarized during sideband cooling, projecting a large fraction of the atoms immediately into the desired state. This is followed by a short optical pumping pulse. As was already observed in Ref. [3], this state decays quickly via dipolar relaxation (arising from the magnetic dipole-dipole interaction between the spins of the valence electrons) to other sublevels within the F=3 manifold. Note that this state is stable against inelastic spin-exchange collisions, since in order to decay it must change its total angular momentum along the magnetic field, which cannot happen via the spherically symmetric ground-state exchange interaction. The magnetic potential energy released in the decay is typically much larger than the depth of our dipole trap, so that the inelastic collision rate coefficient can be easily extracted from the observed time-dependent trap loss rate. This quantity is shown in Fig. 2 vs. magnetic field.

Note the large number of Feshbach resonances, in comparison to the other alkalis where at most one or two have been predicted or observed in a magnetic field range of this size [15–17]. This is due to the much stronger influence of the so-called indirect spin-spin coupling, where the ground state valence electron spins are magnetically coupled via the spin-orbit interaction to distant excited electronic states of the dimer having orbital angular momentum [19]. The result is a coupling of the total electron spin to the molecular axis which breaks the spherical symme-

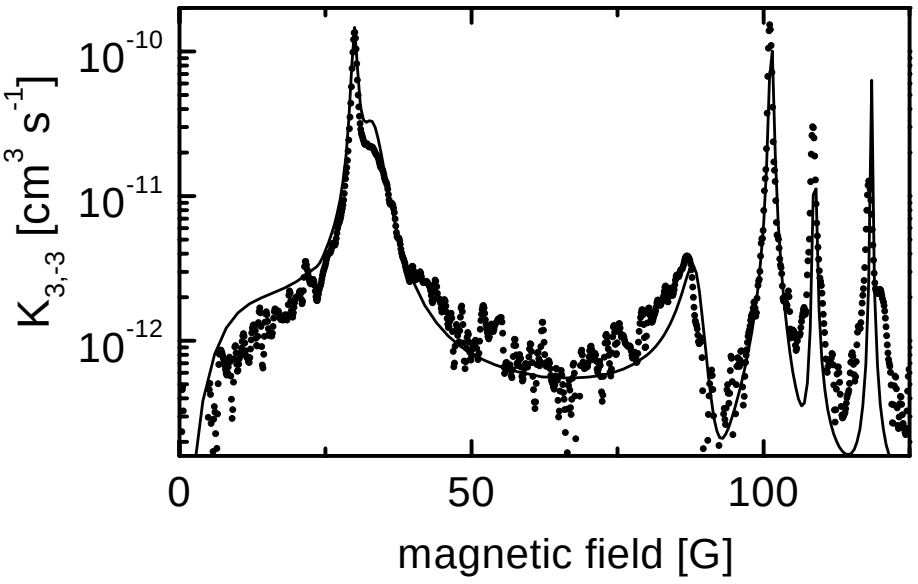

FIGURE 2. Dipolar loss rate coefficient vs. magnetic field for atoms in the $|3,-3\rangle$ state. The solid line is the theoretical curve obtained by fitting to the resonance positions shown in Figs. 1(a), 2, and 3.

try of the ground state molecular interaction in the same way as the well-known ("direct") magnetic dipole-dipole interaction [19], and therefore contributes to the cross-section for dipolar relaxation. For the lighter alkalis this is an extremely small effect, and the already very weak direct contribution dominates these processes, however for Cs_2 the indirect contribution is anomalously large and overwhelms the direct coupling [19,11,12]. This has two important consequences; first, the dipolar relaxation cross-sections are orders of magnitude larger than for the lighter alkalis [3,4]. Second, free Cs atom pairs in S-wave scattering states can couple much more strongly to rotating molecular states of the dimer, and this produces the many narrow Feshbach resonances observed in these relaxation rates. The positions of these resonances provide a direct measurement of the strength of the indirect spin-spin coupling, which has been an important source of uncertainty in the Cs-Cs interaction, and has until now helped to prevent a consistent picture of these interactions from emerging from the available experimental and theoretical information.

Finally, we observe collisions between atoms polarized in the $|4,-4\rangle$ state. The observed rate coefficient vs. magnetic field is shown in Fig. 3. These samples are prepared using a fast field reversal as described above, again followed by optical pumping. Loss from this state occurs mainly via hyperfine-changing collisions, where one or both of the atoms decays through dipolar relaxation to the lower F=3 manifold. Resonances in this state provide an important constraint on the interaction parameters which is complementary to those already described, since collisions in this state involve only the triplet potential, whereas atoms in the

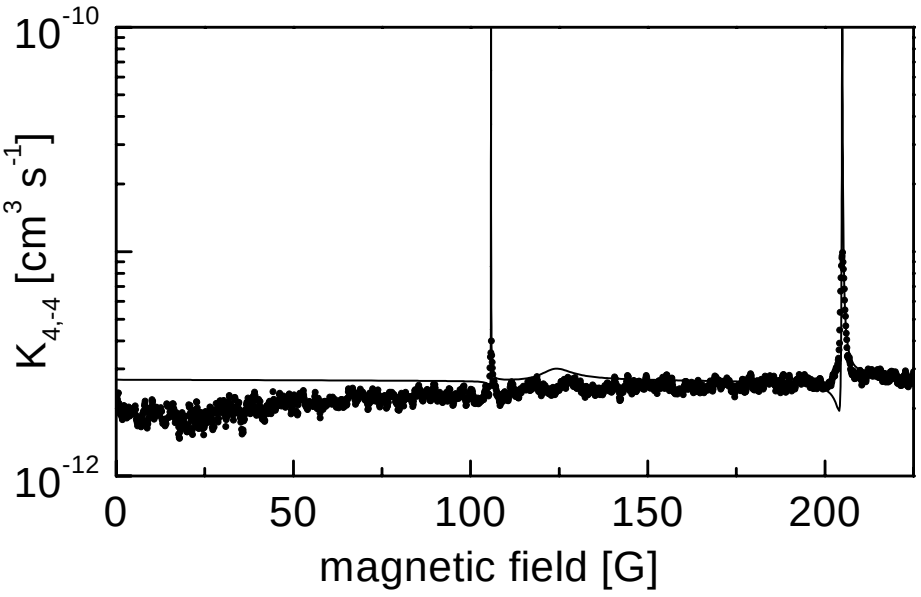

FIGURE 3. Inelastic loss rate coefficient vs. magnetic field for atoms in the $|4,-4\rangle$ state. The solid line is the theoretical curve obtained by fitting to the resonance positions shown in Figs. 1(a), 2, and 3.

lower F=3 manifold experience a mixture of the singlet and triplet potentials. In addition, the bound states responsible for Feshbach resonances in collisions of $|4,-4\rangle$ atoms must have binding energies less than the Zeeman energy of the atom pair, rather than the hyperfine energy as is the case for atoms colliding in the lower F=3 manifold. These extremely weakly bound states are therefore more sensitive to the long-range part of the potential [19].

We use a coupled-channel collision model similar to that described in Refs [11,19] to fit the observed resonance positions shown in Figs. 1(a), 2, 3 [12]. The input to this model are the following four fitting parameters: the singlet and triplet scattering lengths A_s and A_t, the van der Waals coefficient C_6, and a dimensionless scaling factor S_C which controls the strength of the indirect spin-spin interaction [11,12]. The fits are shown as a solid line in Figure 1(b) and in Figs. 2-3 superimposed on the data, and they reproduce the positions of all the observed resonances. The resulting parameter values are A_s = (280 +-10)a_0, A_t = (2400+-100)a_0, C_6 = (6890+-35)a.u., and S_C = 3.2+-0.5. Notice that both the singlet and triplet scattering lengths are positive and very large; these arise from extremely weakly bound states in the singlet and triplet potentials, the latter of which is the source of the zero energy resonance observed in the pure triplet state [2].

In addition to the three spectra shown in Figs. 1(a), 2, and 3, which were taken with spin-polarized samples and were used to extract values for the interaction parameters, we have also observed many additional Feshbach resonances in collisions between atoms in different magnetic sublevels, where P-wave collisions are possi-

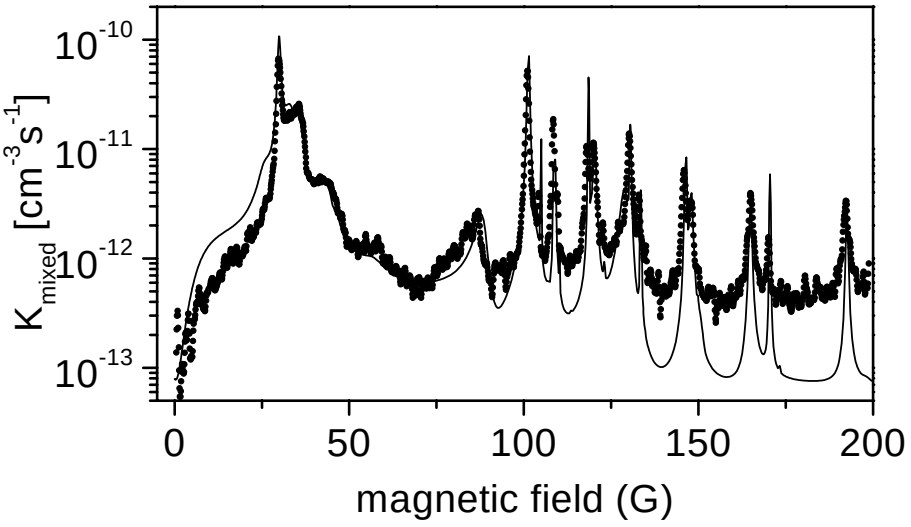

FIGURE 4. Inelastic loss rate coefficient vs. magnetic field for a mixed sample with 70% $|3,-3\rangle$, 25% $|3,-2\rangle$, and 5% $|3,-1\rangle$. Note that many of the additional features are due to P-wave collisions between atoms in different sublevels. The solid line is the theoretical curve obtained by fitting to the resonance positions shown in Figs. 1(a), 2, and 3.

ble. A detailed presentation of these spectra and resonance positions is beyond the scope of this paper, and will be presented elsewhere. However, we give an example in Fig 4. This figure shows the observed inelastic loss for a sample of atoms in a mixture of the $|3,-3\rangle$, $|3,-2\rangle$, and $|3,-1\rangle$ states, which was obtained simply by imperfectly polarizing the gas. All additional resonances are correctly reproduced by the calculations, whose only input is the four parameters extracted from Figs. 1(a), 2, and 3.

We now call the reader's attention to the small resonances predicted in the elastic cross section for $|3,3\rangle$ atom collisions, which are magnified in the inset of Fig. 1, and are clearly too weak to be seen in the evaporative loss. In order to observe these features, we use optical excitation to probe the short-range molecular formation characteristic of Feshbach resonance [17]. A free atom pair within an optical wavelength of each other experiences a very strong, spatially dependent shift of the electronic transition frequency due to the resonant-dipole interaction in the excited state. A light field at a certain detuning will thus be resonant only at a particular interatomic distance, called the Condon point Rc, and the excitation probability is proportional to the probability density with which atoms are found at that particular separation [20]. Excited pairs can undergo a so-called radiative collision, where the tremendously strong dipole forces in the excited state accelerate the atoms to a sufficiently high kinetic energy before they decay that they are expelled from the trap [20,7]. By monitoring the light-induced loss from our trap at a suitable detuning (in this case 6 nm above resonance), we can directly probe

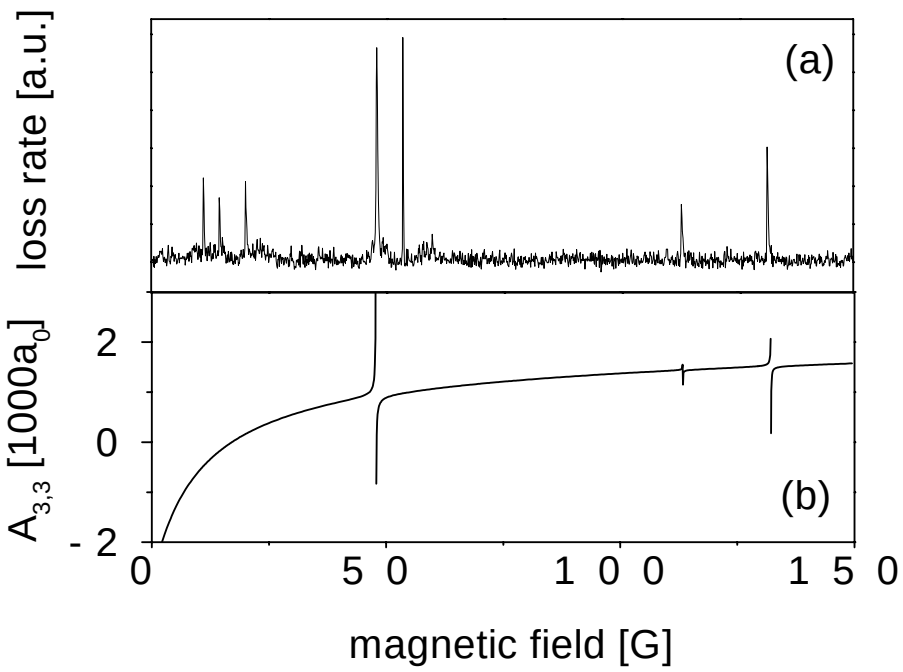

FIGURE 5. (a) Radiative collision loss rate vs. magnetic field for atoms in the $|3,3\rangle$ state. (b) Calculated scattering length $A_{3,3}$, showing the predicted Feshbach resonances. Note that even the very weak features are clearly seen in the loss rate. Several of the observed resonances are not predicted, and may be due to higher-oder scattering processes.

atomic pair correlation function at a small interatomic distance characteristic of molecular formation, and thus sensitively detect the resonant enhancement of this quantity which occurs at a Feshbach resonance. Figure 5(a) shows the observed radiative collision loss for atoms in the $|3,3\rangle$ state as a function of magnetic field, and Figure 5(b) shows the predicted scattering length of this state for comparison of the resonance positions. Both of the weak features predicted by the calculations appear clearly in the radiative loss rate, as well as the larger resonance at 48 G already observed in the evaporative loss. Note also that several additional features are also present which were not predicted by the theory. We are currently investigating the possibility that these resonances result from higher order processes where the incoming S-wave couples to rotating molecular states of even higher angular momentum (e.g. l=4,6 etc...), and the agreement appears to be promising. This will be the subject of a future publication.

With a consistent set of ultracold molecular interaction parameters, we can now calculate the rates for arbitrary cold collision processes. Of particular interest is the cold-collision induced frequency shift of the so-called "clock transition" between $|3,0\rangle$ and $|4,0\rangle$, which is likely to be the most important limitation on the short-term stability of the next generation of laser-cooled cesium atomic fountain clocks [5,21].

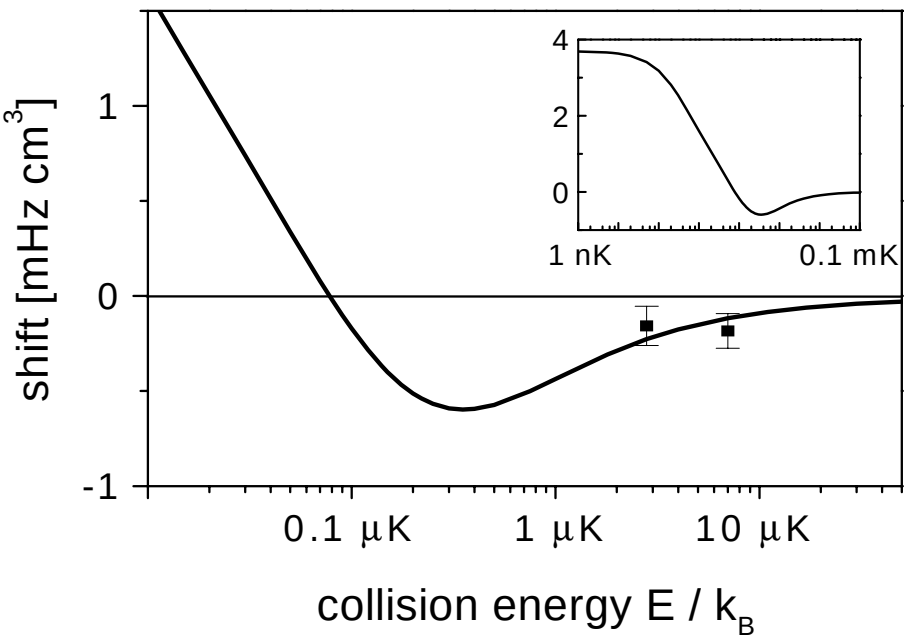

FIGURE 6. (a) Cold-collision induced frequency shift of the $|3,0\rangle$ to $|4,0\rangle$ transition calculated for an equal mixture of these two states, as a function of collision energy. The existing experimental points are shown, and agree with the calculation. Note that the shift goes through zero at about 90 nK.

Shown in Fig. 6 is the calculated frequency shift per unit density, as a function of the atomic kinetic energy in temperature units. Also shown are several experimental points from Ref. [5], which are in good agreement with the calculation. Notice that the curve passes through zero and changes sign at a temperature of about 90 nK. If a large enough sample of atoms could be produced in a narrow energy range around this point, it might be possible to dramatically reduce the effect of this density-induced shift [21]. 3D Raman-sideband cooling [18] has already been used to produce an atomic fountain with 10^8 atoms at temperatures as low as 150 nK [22], and would therefore be a very promising technique for this purpose.

As a second and final example of what can be calculated using the interaction parameters, we now consider the impact this new information has on attempts to produce a cesium Bose-Einstein condensate. Shown in Fig. 7 are the calculated elastic and inelastic collision rate coefficients for atoms in the $|3,-3\rangle$ state, where experimental efforts at BEC in a magnetic trap have been focused [3,4]. The ratio of these two quantities R is a figure of merit for forced evaporative cooling [23]. Although R takes on values of 100 or larger away from the resonances, there are additional considerations that are important. First, the sign of the scattering length must be positive, at least during the final evaporation stages where $T \leq T_c$, to have

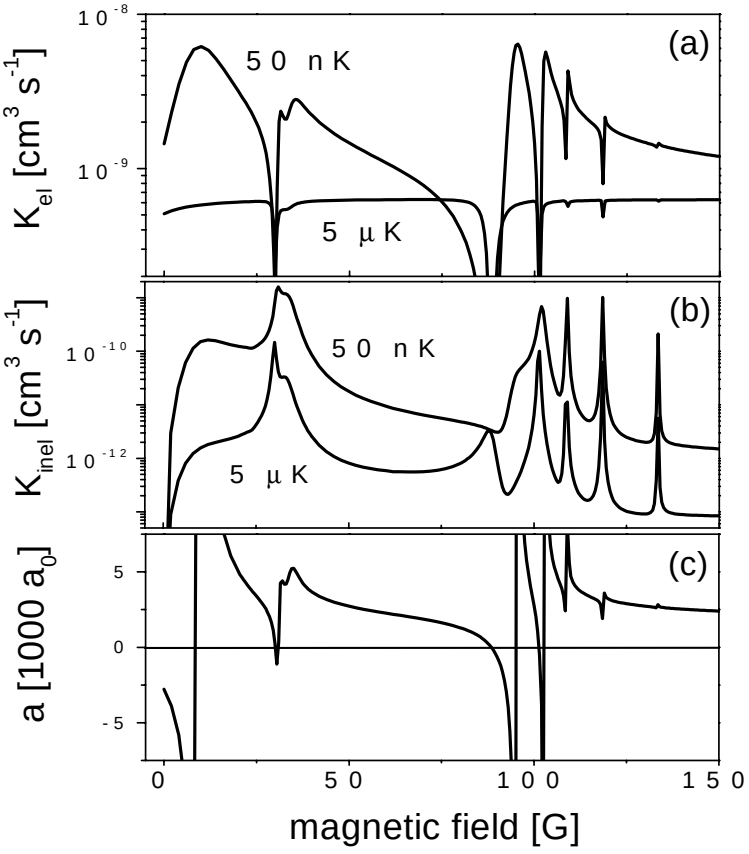

FIGURE 7. For atoms in the $|3,-3\rangle$ state, the calculated elastic collision rate coefficient is shown in (a), the inelastic collision rate coefficient in (b), and the scattering length in (c). The collision rate coefficients are orders of magnitude larger than typically seen in the lighter alkalis; also, the scattering length for $|3,-3\rangle$ is large and negative in the low-field region where evaporation was performed in Ref [4].

a large, stable condensate. This eliminates the region below about 10G, where the previous experiments were performed [3,4]. Second, the absolute magnitudes of these rate coefficients are enormous. This is important because the trap vibration period and trap lifetime are fixed timescales against which elastic and inelastic rates must be compared absolutely, rather than just to each other. Inelastic loss rates must be kept small enough so that one has sufficient time to observe the condensate, and elastic collision rates larger than the trap vibration frequency cause a crossover into hydrodynamic behavior. The latter may be a serious problem for evaporation, either by limiting the thermalization rate [6] or by reducing the evaporation efficiency or dimensionality. These effects must be characterized before an intelligent choice of parameters can be made based upon our measurements.

In conclusion, we have presented high-resolution spectra of elastic and inelastic

collision rates in an ultracold, trapped cesium gas. From these spectra we have for the first time extracted a self-consistent set of molecular interaction parameters which reproduce the positions of over 30 observed Feshbach resonances. These parameters can be used to accurately calculate important collisional effects such as the density-dependent frequency shift in cesium atomic clocks, as well as collision rates and scattering lengths relevant for attempts at Bose-Einstein condensation. In addition, Feshbach spectroscopy may be more widely useful as a general spectroscopic tool for studying cold collisions, especially when optical excitation is used as a sensitive probe of the molecular formation.

ACKNOWLEDGMENTS

This work was supported in part by grants from the AFOSR and the NSF. V.V. would like to acknowledge support from the Humboldt Foundation and C.C. from the Taiwan government.

REFERENCES

1. C.R. Monroe, E.A. Cornell, C.A. Sackett, C.J. Myatt, and C.E. Wieman, *Phys Rev. Lett.* **70**, 414 (1993); S.A. Hopkins, S. Webster, J. Arlt, P. Bance, S. Cornish, O. Marago, and C.J. Foot, *Phys Rev. A* **61**, 032707 (2000); R. Legere and K. Gibble, *Phys Rev. Lett.* **81**, 5780 (1998); K. Gibble, S. Chang, and R. Legere, *Phys Rev. Lett.* **75**, 2666 (1995).
2. M. Arndt, M. Ben-Dahan, D. Guéry-Odelin, M.W. Reynolds, and J. Dalibard, *Phys Rev. Lett.* **79**, 625 (1997).
3. J. Söding, D. Guéry-Odelin, P. Desbiolles, G. Ferrari, and J. Dalibard, *Phys Rev. Lett.* **80**, 1869 (1998).
4. D. Guéry-Odelin, J. Söding, P. Desbiolles, and J. Dalibard, *Opt. Express* **2**, 323 (1998); D. Guéry-Odelin, J. Söding, P. Desbiolles, and J. Dalibard, *Europhys. Lett.* **44**, 25 (1998).
5. K. Gibble and S. Chu, *Phys Rev. Lett.* **70**, 1771 (1993); S. Ghezali, Ph. Laurent, S.N. Lea, and A. Clairon, *Europhys. Lett.* **36**, 25 (1996); G. Santarelli, Ph. Laurent, P. Lemonde, A. Clairon, A.G. Mann, S. Chang, A.N. Luiten, and C.Salomon, *Phys Rev. Lett.* **82**, 4619 (1999).
6. V. Vuletić, A.J. Kerman, C. Chin, and S. Chu, *Phys Rev. Lett.* **82**, 1406 (1999).
7. V. Vuletić, C. Chin, A.J. Kerman, and S. Chu, *Phys Rev. Lett.* **83**, 943 (1999).
8. C. Chin, V. Vuletić, A.J. Kerman, and S. Chu, *Phys Rev. Lett.* **85**, 2717 (2000).
9. B.J. Verhaar, K. Gibble, and S. Chu, *Phys Rev. A* **48**, R3429 (1993); K. Gibble and B.J. Verhaar, *Phys. Rev. A* **52**, 3370 (1995); S.J.J.M.F. Kokkelmans, B.J. Verhaar, and K. Gibble, *Phys Rev. Lett.* **81**, 951 (1998).
10. E. Tiesinga, A.J. Moerdijk, B.J. Verhaar, and H.T.C. Stoof, *Phys. Rev. A* **46**, R1167 (1992); E. Tiesinga, B.J. Verhaar, and H.T.C. Stoof, *Phys. Rev. A* **47**, 4114 (1993).
11. P.J. Leo, E. Tiesinga, P.S. Julienne, D.K. Walker, S. Kadlecek, and T.G. Walker, *Phys Rev. Lett.* **81**, 1389 (1998).

12. P.J. Leo, C.J. Williams, and P.S. Julienne, *Phys Rev. Lett.* **85**, 2721 (2000).
13. M. Bijlsma, B.J. Verhaar, and D.J. Heinzen, *Phys. Rev. A* **49**, R4285 (1994); C. Chin, V. Vuletić, V. Leiber, A.J. Kerman, and S. Chu, Accepted to *Phys. Rev. A*
14. H. Feshbach, it Ann. Phys. (N.Y.) **19**, 287 (1962).
15. J. Bohn, J.P. Burke, C.H. Greene, H. Wang, P.L. Gould, and W.C. Stwalley, *Phys. Rev. A* **59**, 3660 (1999); J.M. Vogels, C.C. Tsai, R.S. Freeland, S.J.J.M.F. Kokkelmans, B.J. Verhaar, and D.J. Heinzen, *Phys. Rev. A* **56**, R1067 (1997); H.M.J.M. Boesten, J.M. Vogels, J.G.C. Tempelaars, and B.J. Verhaar, *Phys. Rev. A* **54**, R3726 (1996); M. Houbiers, H.T.C. Stoof, W.I. McAlexander, and R.G. Hulet, *Phys. Rev. A* **57**, R1497 (1998).
16. S. Inouye, M.R. Andrews, J. Stenger, H.-J. Miesner, D.M. Stamper-Kurn, and W. Ketterle, *Nature (London)* **392**, 151 (1998); J.L. Roberts, N.R. Claussen, J.P. Burke, C.H. Greene, E.A. Cornell, and C.E. Wieman, *Phys. Rev. Lett.* **81**, 5109 (1998);
17. Ph. Courteille, R.S. Freeland, D.J. Heinzen, F.A. van Abeelen, and B.J. Verhaar, *Phys. Rev. Lett.* **81**, 69 (1998).
18. A.J. Kerman, V. Vuletić, C. Chin, and S. Chu, *Phys. Rev. Lett.* **84**, 439 (2000).
19. F.H. Mies, C.J. Williams, P.S. Julienne, and M. Krauss, *J. Res. Natl. Inst. Stand. Technol.* **101**, 521 (1996).
20. K. Burnett, P.S. Julienne, and K.-A. Suominen, *Phys. Rev. Lett.* **77**, 1416 (1996).
21. P.J. Leo, P.S. Julienne, F.H. Mies, and C.J. Williams, Submitted to *Phys. Rev. Lett.*
22. P. Treutlein, KY. Chung, and S. Chu, submitted to *Phys. Rev. Lett.*
23. W. Ketterle and N.J. van Druten, *Adv. At. Mol. Opt. Phys.* **37**, 181 (1996) and references therein